Effect of the Uneven Circumferential Blade Space on the Performance of Small Axial Flow Fan

LIU Yang[1], LIN Zhe[1], LIN Peifeng[1], JIN Yingzi[1*], Toshiaki Setoguchi[2], Heuy Dong Kim[3]

1. Key Laboratory of Fluid Transmission Technology of Zhejiang Province, Zhejiang Sci-Tech University, Hangzhou 310018, China
2. Department of Mechanical Engineering, Saga University, Honjo-machi, Saga, 840-8502, Japan
3. School of Mechanical Engineering, Andong National University, Seongcheon-Dong1375, Gyeongdong-RD, Andong, Gyeongsangnuk-DO, 760-749, Korea

Effects of the uneven circumferential blade space on static characteristics and aerodynamic noise of a small axial flow fan are studied in this work. The blade angle modulation is adopted to design a series of unequally spaced fans, which have different maximum of modulation angular displacement. The steady flow is simulated by the calculations of Navier-Stokes equations coupled with RNG k-epsilon turbulence model, while the unsteady flow is computed with large eddy simulation. According to theoretical analysis, a fan with a maximum of modulation angular displacement of 6° is regarded as the optimal unequally spaced fan. The experiment of static characteristic is carried out in a standard wind tunnel and the aerodynamic noise of both fans is tested in a semi-anechoic room. Then, performances of the optimal unequally spaced fan are compared with those of the prototype fan. The results show that there is reasonable agreement between the simulation results and the experimental data. It is found that the discrete noise of the optimal unequally spaced fan is lower than that of the prototype fan at the near field monitoring point. This can be explained that the total pressure fluctuation of the optimal unequally spaced fan is much more regular than that of the prototype fan.

Keywords: small axial flow fan, uneven circumferential blade space, static characteristics, discrete noise, broadband noise

Introduction

The aerodynamic noise of axial flow fan is usually composed of discrete noise and broadband noise. The discrete noise is generated by the rotating blades punching the air particle periodically, whose spectrum shows for a series of discrete noise peaks. The discrete frequency depends on the blade number of the fan, rotational speed and tonal characteristics. It may be more annoying than broadband noise in some situations [1]. Therefore, the noise environment of axial flow fan can be improved effectively by reducing the discrete noise.

Blades are distributed unevenly in the circumferential direction as a passive method to reduce the discrete noise of axial flow fan has first been suggested by Mellin et al. [2] and continuously developed and applied. Sun [3] derived the acoustic radiation formula of unequally spaced fan according to BLH (Blade Loading Harmonics) theory

JIN Yingzi: Professor
This work was supported by National Natural Science Foundation of China (No. 51276172), ZSTUME01A04 and 2013TD18 etc..

presented by Wright [4], and further elucidated the reasons for reducing noise through this method. Besides, Sun believed that the blade space variation of fans in a large range wouldn't have the obvious effect on the aerodynamic performance of axial flow fan. Cui [5] applied this method on the fan for mines, and compared the actual effect of blade number on noise reduction in the tunnel. The result showed that the noise reduction of unequally spaced fan with singular blades was much larger than that of unequally spaced fan with even blades. The studies by Xu [6] showed that unequally spaced fan not only eliminated the well-regulated pressure destabilization caused by the equally spaced blades, but also weakened the resonance noise generated by the interference between the blades and the fixed obstacles in the ventilating duct, thus reducing the discrete noise of fans.

In the present work, the uneven circumferential blade space was applied on the small axial flow fan to reduce the noise. The application is successful and the research results are benefit for parameter optimization and noise prediction of unequally spaced small axial flow fan.

Research method

Design of unequally spaced fan

At present, the design method of unequally spaced fan can be divided into four groups: look-up table [2], convert to two-bladed-propellers [7-8], blade angle modulation [9-12] and trial calculation method [1]. In this paper, blade angle modulation was adopted to design a series of unequally spaced fans. The method has first been proposed by Ewald et al. [9] and improved by Duncan and Dawson [10]. Fiagbedzi [11] thoroughly analyzed it mathematically. Roger [12] provided a more physical analysis. The method consists of varying the blade space according to:

$$\theta_i' = \theta_i + \Delta\theta \sin(n\theta_i) \qquad (1)$$

As shown in Fig. 1, the coordinate system was established to determine the angular position of each blade, the center of the axial flow fan was regarded as the original point and the angular position of *z*th blade was regarded as the reference 0°. The angle θ_i is the angular position of *i*th blade of equally spaced fan, θ_i' is the angular position of *i*th blade of unequally spaced fan, $\Delta\theta$ is the maximum of modulation angular displacement, and n is the cycle index of modulation. Besides, blades of the fan are balanced naturally when n≥2.

Based on Eq. (1), we can conclude that the larger $\Delta\theta$ is, the more uneven distribution of blades in the circumferential direction. Thus, the difference of performance between equally spaced fan and unequally spaced fan becomes more remarkable. Therefore, it's very important to select a reasonable $\Delta\theta$ by considering static characteristics and aerodynamic noise of axial flow fan reasonably.

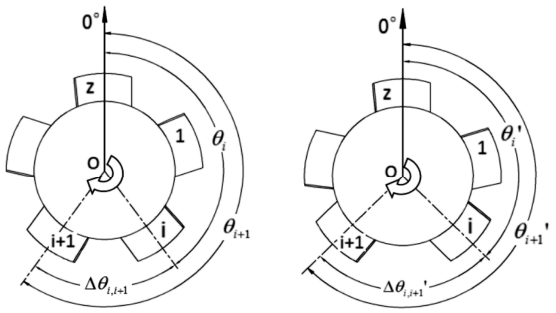

(a) Equally spaced fan (b) Unequally spaced fan

Fig. 1 Schematic of coordinate system.

Simulation for static characteristics

The steady flow was simulated by the calculations of Reynolds averaged Navier-Stokes equations coupled with RNG k-epsilon turbulence model. The standard wall function was used to deal with the regions near the wall. The SIMPLE algorithm was adopted to carry on the coupling between pressure and velocity. The second order upwind difference scheme was selected to discrete the governing equations. The computational domain of the fans (see Fig. 2) is divided into the inlet region, the outlet region, the rotating fluid region and the casing region. The inlet region is a hemisphere with radius r = 85 mm. The outlet region is a cylinder with radius R = 170 mm and extends to 500mm to ensure that the fluid through the fan has been fully developed. The mass flow rate at the inlet was controlled and the pressure at the outlet was set to atmospheric pressure.

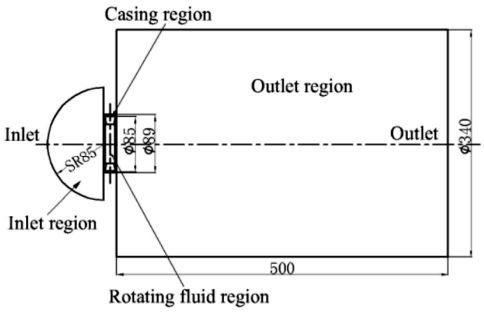

Fig. 2 Computational domain of fans.

Simulation for aerodynamic noise

The large eddy simulation and Ffowcs Williams-Hawkings (FW-H) noise model were adopted for unsteady simulation and aerodynamic noise prediction. The solution obtained by the steady simulation at the rated condition (Q = 0.01 kg/s) was regarded as the initial condition of large eddy simulation. The finite volume method was used to disperse the filtered Navier-Stokes equations. The PISO algorithm was applied for the coupling between pressure and velocity. The second order central difference scheme was selected to couple the momentum

equation. In order to solve the interaction of interfaces, the dynamic grid method was used in the interfaces between the rotating fluid region and the casing region.

Selection of optimal unequally spaced fan

The small axial flow fan used in this work is shown in Fig. 3, whose main parameters are listed in Table 1. The angular position of each blade of the prototype fan in the coordinate system as shown in Fig. 1 is listed in Table 2.

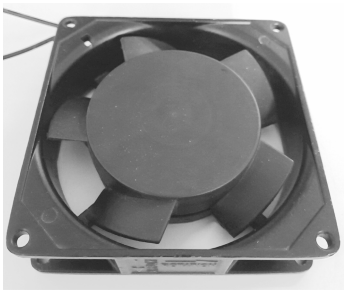

Fig. 3 Prototype fan.

Table 1 Main parameters of prototype fan

Main parameters	Value
External diameter (mm)	85
Hub ratio	0.72
Stagger angle (°)	27.7
Blade number	5
Tip clearance (mm)	2
Rated condition (kg/s)	0.01
Rated rotational speed (r/min)	3000

Table 2 Angular position of each blade of prototype fan

Blade i	1	2	3	4	5
θ_i (°)	72	144	216	288	360(0)
$\Delta\theta_{i,\,i+1}$ (°)	72	72	72	72	72

On the basis of the prototype fan, a series of unequally spaced fans with different Δθ were designed according to the blade angle modulation. Fig. 4 shows the variation of static pressure with Δθ, the solid black line is plotted in the light of static pressure data of different fans by means of the least square method. It can be seen from the figure that the static pressure of the fans first increases and then decreases in general with the increase of Δθ at the rated condition. The 4% drop of static pressure of the prototype fan as shown in Fig. 4 is regarded as the acceptable range, and this standard can be adjusted according to the actual situation. Therefore, the fans with Δθ≤22° can meet the requirements.

Fig. 5 shows the variation of efficiency with Δθ, and the solid black line is plotted in the light of efficiency data of different fans by means of the least square method. It can be observed from the figure that the efficiency of the fans decreases in general with the increase of Δθ at the rated condition. The 4% drop of efficiency of the prototype fan as shown in Fig. 5 is regarded as the acceptable range, and this standard also can be adjusted according to the actual situation. Thus, the fans with Δθ≤8° can meet the requirements.

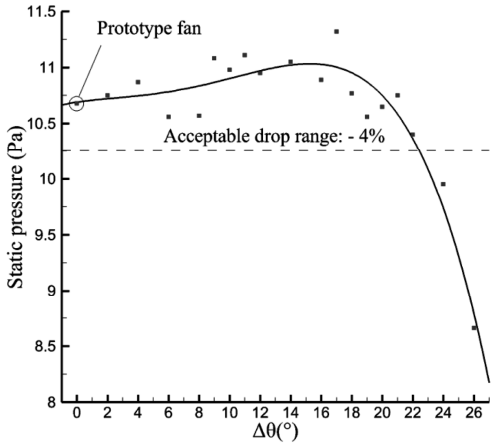

Fig. 4 Variation of static pressure with Δθ.

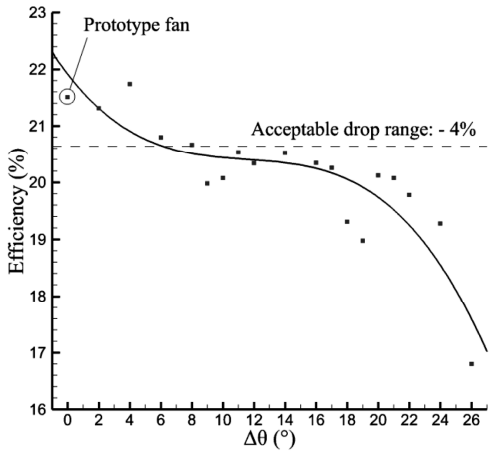

Fig. 5 Variation of efficiency with Δθ.

A near field monitoring point and a far field monitoring point were set at the positions of 1mm and 1m away from the impeller hub on the positive rotational axis, respectively. Fig. 6 shows the variation of Sound Pressure Level (SPL) with Δθ at both monitoring points at the rated condition. Compared to the prototype fan, unequally spaced fans with different Δθ make SPL reduced at the near field monitoring point and have little variation at the far field monitoring point. It's worth noting that although the larger Δθ makes the distribution of blades in the circumferential direction more uneven, SPL at the near field monitoring doesn't decrease monotonously with the increase of Δθ, but fluctuates in a certain range.

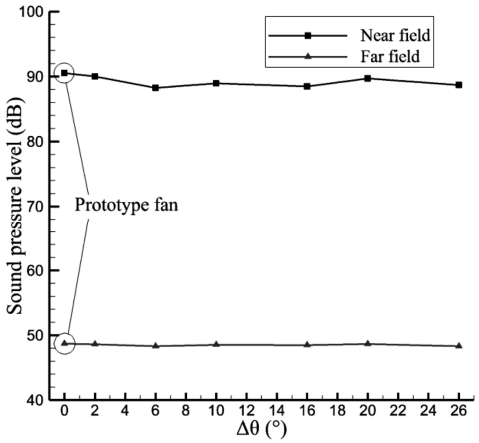

Fig. 6 Variation of SPL with Δθ.

Table 3 Angular position of each blade of optimal unequally spaced fan

Blade i	1	2	3	4	5
θ_i'(°)	75.5	138.3	221.7	284.5	360
$\Delta\theta_{i,i+1}'$(°)	62.76	83.42	62.76	75.53	75.53
$\frac{\Delta\theta_{i,i+1}'-\Delta\theta_{i,i+1}}{\Delta\theta_{i,i+1}}\times100(\%)$	-12.8	15.9	-12.8	4.9	4.9

Taking into account the static characteristic and the aerodynamic noise of these fans reasonably, a fan with Δθ = 6° is regarded as the optimal unequally spaced fan. By means of Eq. (1), the design equation is written as:

$$\theta_i' = \theta_i + 6\sin(2\theta_i) \tag{2}$$

The angular position of each blade of the optimal unequally spaced fan is listed in Table 3. According to the verification of Eqs.(3),

$$\begin{cases} \sum_{i=1}^{5} \sin\theta_i' = 0 \\ \sum_{i=1}^{5} \cos\theta_i' \approx 0.0067 \approx 0 \end{cases} \tag{3}$$

the center of mass of the optimal unequally spaced fan is still kept on the rotational axis. Thus, the rotational vibration due to eccentricity would not appear. It can be seen from the angle between the adjacent blades in Table 3 that the unequally spaced fan designed by blade angle modulation still retains a certain degree of symmetry. Compared to the prototype fan, the maximum variation of space in the circumferential direction occurs between blade 2 and blade 3, whose variation rate reaches to 15.9%, which is consistent with Ref. [4] in which a range less than 20% is recommended.

Comparison of static characteristics

Simulation results and analysis

Static characteristics of small axial flow fan are the basic indexes to evaluate the quality of fans. Fig. 7 shows comparisons of static characteristic curves between the optimal unequally spaced fan and the prototype fan, including static pressure (P-Q) curve in Fig. 7(a) and efficiency (η-Q) curve in Fig. 7(b). The same variation tendency of P-Q curves of both fans is shown in Fig. 7(a). The static pressure decreases sharply at first, then increases slowly and finally decreases rapidly with the increase of flow rate. Besides, the values of static pressure of the optimal unequally spaced fan and the prototype fan are close to each other at different flow rate. The stable operation condition of both fans is from 0.005kg/s to 0.012kg/s. Once beyond this range of flow rate, static pressure will change dramatically.

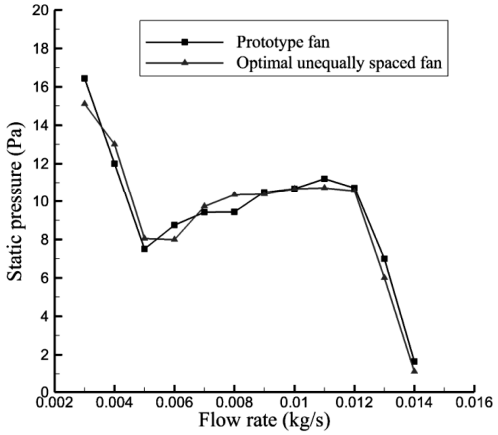

(a) P-Q curve

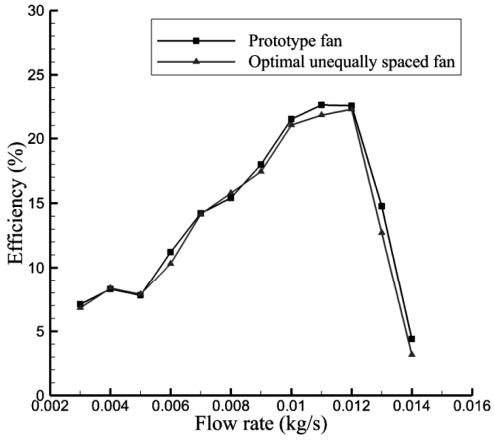

(b) η-Q curve

Fig. 7 Static characteristic curves.

In Fig. 7(b), η-Q curves of both fans also show the same variation tendency. The efficiency increases slowly at first, and finally decreases rapidly. The maximum of efficiency exceeds 22%. The values of efficiency of both fans are close to each other in a certain range of flow rate. Moreover, the prototype fan has the maximum efficiency in Q = 0.011 kg/s while the optimal unequally spaced fan

has the maximum efficiency in Q = 0.012 kg/s.

Fig. 8 is the static pressure contour on the surface of impellers at the rated condition. By comparing Fig. 8(a) and (b), it is found that the values and distributions of static pressure of the optimal unequally spaced fan and the prototype fan are similar on the suction side of blades in general. The negative pressure zones around -40 Pa and -50 Pa were appeared in most of the blades. The former is located in the middle of the blade and the latter is near the leading edge of the blade. By comparing Fig. 8(c) and (d), the static pressure zone above 20 Pa appears on the surface of a few blades on the pressure side, but the values and distributions of static pressure are also similar. The difference of the static pressure field between the optimal unequally spaced fan and the prototype fan is very little which can be used to explain the similar P-Q curve.

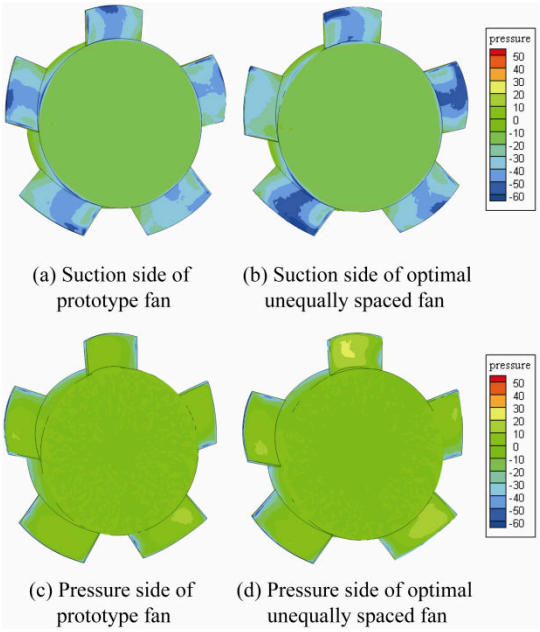

Fig. 8 Static pressure contour on the surface of impellers.

Wind tunnel experiment

In order to verify the reliability of simulation, static pressure of the optimal unequally spaced fan and the prototype fan was tested in the wind tunnel as shown in Fig.9. The experimental fans are shown in Fig. 10.

Fig. 11 shows the comparison of P-Q curve of the prototype fan between simulation and experiment. The results of simulation and experiment are in good agreement with each other, especially at the stable operation condition ranging from 0.005 kg/s to 0.011 kg/s. Thus, the reliability of the simulation is confirmed.

Fig. 12 shows the experimental results of P-Q curve of the optimal unequally spaced fan and the prototype fan. The variation tendency of P-Q curves of both fans is almost the same. The static pressure decreases sharply at

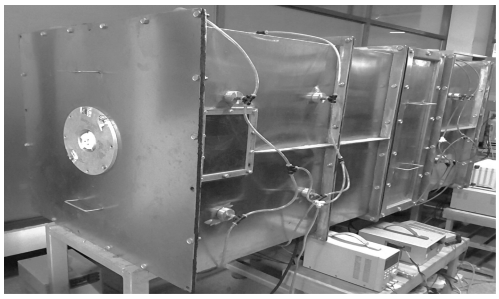

Fig. 9 Wind tunnel used for the experiments.

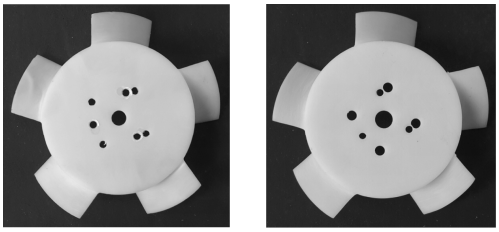

(a) Prototype fan (b) Optimal unequally spaced fan

Fig. 10 Experimental fans.

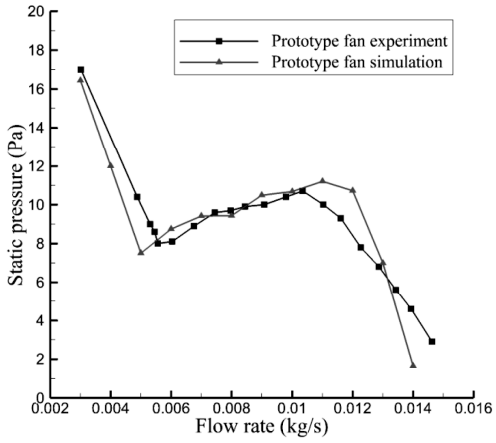

Fig. 11 Comparison of P-Q curve of prototype fan between simulation and experiment.

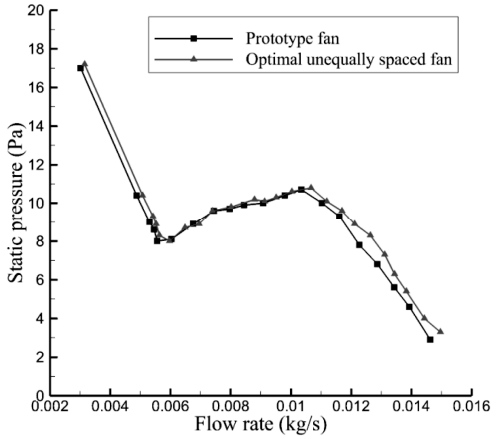

Fig. 12 Experimental results of P-Q curve of both fans.

first, then increases slowly and finally decreases rapidly with the increase of flow rate. Moreover, the differences of static pressure between both fans are little at the stable operation condition ranging from 0.005 kg/s to 0.011 kg/s. Combined with simulation and wind tunnel experiment, it can be concluded that the optimal unequally spaced fan has a little change on static characteristics of the prototype fan.

Comparison of aerodynamic noise

Simulation results

Fig. 13 shows the variation of SPL with the time for the optimal unequally spaced fan and the prototype fan at both monitoring points. Before the fans rotate 6T (T is the rotational period of the fan), SPL at the near field monitoring point and the far field monitoring point are both unstable, showing an overall downward trend. After the fans rotate 6T, SPL at both monitoring points remains almost unchanged, indicating that the internal flow field of the fans reaches the relatively steady state at this moment. At the near field monitoring point, the noise reduction of the optimal unequally spaced fan is more than 2dB compared to the prototype fan, but at the far field monitoring point, the effect of noise reduction of the optimal unequally spaced fan is not obvious. Generally, the attenuation of discrete noise is faster than that of broadband noise. It can be considered that the noise at the near field monitoring point is dominated by discrete noise and the noise at the far field monitoring point is dominated by broadband noise. Therefore, it can be concluded preliminarily that the uneven circumferential blade space can reduce discrete noise of small axial flow fan obviously, but the effect on broadband noise is very little.

Fig. 14 shows SPL along the axial direction in the downstream of fans. It is found that SPL of the optimal unequally spaced fan is lower than that of the prototype fan at all axial positions. The largest difference is located at the near field monitoring point and is up to 2.3dB. The difference of SPL between both fans becomes smaller with the increase of axial distance between the monitoring point and the fan. When the axial distance exceeds 600 mm, their difference is stable and reaches to 0.4dB. Due to attenuation speed of discrete noise is much faster than broadband noise, we can conclude that when the axial distance exceeds 600 mm, the discrete noise has been completely attenuated and the broadband noise is dominant. The attenuation process of the discrete noise can be observed clearly in Fig. 14 which further proves that the uneven circumferential blade space can reduce discrete noise of small axial flow fan obviously, but the effect on broadband noise is very little.

Fig. 15 shows distributions of Power Spectral Density (PSD) at the near field monitoring point. The prototype

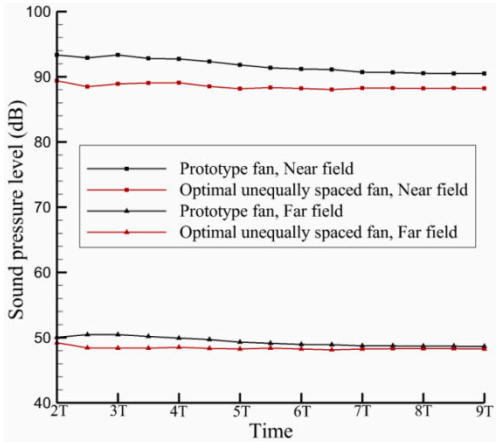

Fig. 13 Variation of SPL with the time at both monitoring points.

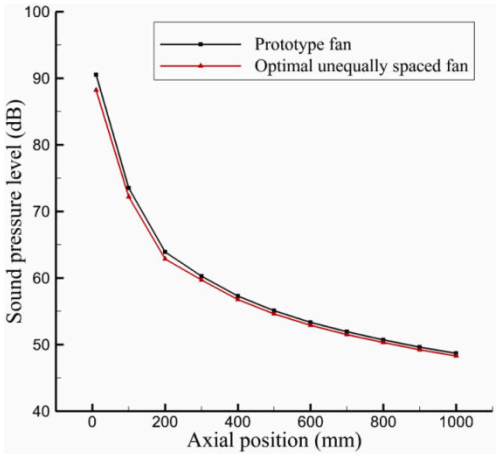

Fig. 14 SPL along the axial direction in the downstream of fans.

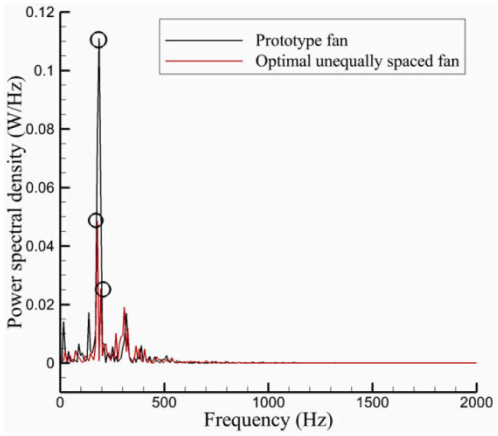

Fig. 15 Distributions of PSD at the near field monitoring point.

fan has a peak in 200 Hz whose value is 0.11 W/Hz. The optimal unequally spaced fan divides this peak into two lower peaks whose values are 0.05 W/Hz and 0.025

W/Hz, which means that the optimal unequally spaced fan does not reduce the total acoustic wave energy in 200 Hz, but makes the energy spread in the frequency domain. When the frequency exceeds 600 Hz, the PSD of both fans tends to zero. The noise reduction of the optimal unequally spaced fan at the near monitoring point mainly concentrates on 200 Hz, which further proves that the reduced noise is discrete noise.

Fig. 16 shows SPL of 1/3 octave band at the far field monitoring point. It can be seen from the figure that the band of the highest SPL ranges from 200 Hz to 250 Hz and the highest SPL reaches to 40dB. The optimal unequally space fan moves the highest SPL ranges to the higher frequency ranging from 300 Hz to 360 Hz, but the value of the highest SPL is unchanged. In the rest of the band, the values of SPL of both fans are close to each other. Therefore, the effect on the broadband noise reduction of the optimal unequally spaced fan at the far field monitoring point is very little.

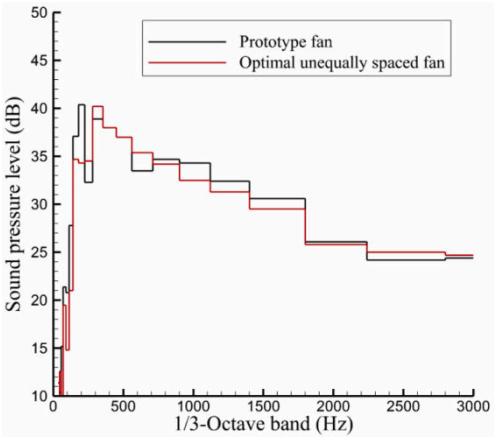

Fig. 16 SPL of 1/3 octave band at the far field monitoring point.

Analysis of flow field characteristics

As we known, the uneven circumferential blade space can reduce discrete noise of small axial flow fan obviously, but the effect on broadband noise is very little. In this section, the reasons will be explained from the view of flow field characteristics.

Fig. 17 shows the total pressure fluctuation of the optimal unequally spaced fan and the prototype fan at the near field monitoring point. According to the above section, both fans reach a relatively stable state after rotating 6T. So the total pressure fluctuation during the time ranging from 6T to 9T is selected here. The total pressure fluctuation of both fans does not show the obvious periodic variation even appears about four peaks in each rotational period. This is the reason why the frequency of the peak of PSD is 200 Hz at the near field monitoring point. Compared to the prototype fan, the total pressure fluctuation of the optimal unequally spaced fan is more like an equal amplitude oscillations and the extreme difference of fluctuation is smaller.

Fig. 18 shows the total pressure fluctuation at the position 500 mm away from the impeller hub on the positive rotational axis. It can be seen from the figure that the total pressure fluctuation of the optimal unequally spaced fan and the prototype fan is irregular at this position. Besides, the values of the total pressure fluctuation are very small. Therefore, the noise at this position is not affected by the total pressure fluctuation. Since the far field monitoring point is further away from the impeller hub, these explanations can also be applied to the far field monitoring points.

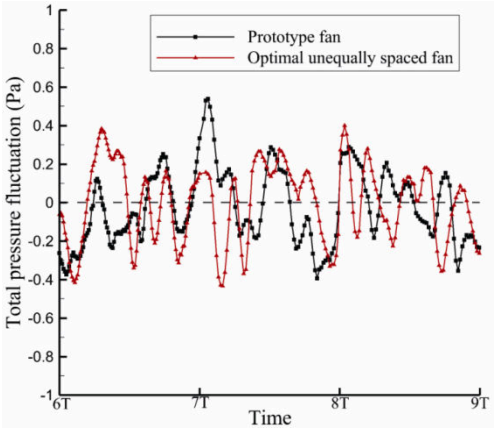

Fig. 17 Total pressure fluctuation at the near field monitoring point.

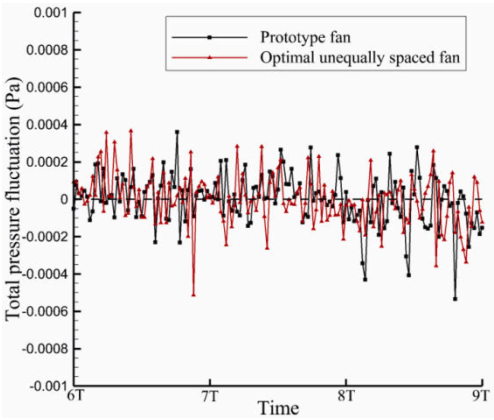

Fig. 18 Total pressure fluctuation at the position 500mm away from impeller hub on the positive rotational axis.

Fig. 20 shows the vorticity contours at the section Z = 6 mm at different moments, where the vorticity contours at the moment of 7T, 7T+3T/5 and 8T are regarded as the representatives. The section Z = 6 mm is near the trailing edge of blades as shown in Fig. 19. By comparing Fig. 20(a) and (b), (c) and (d), (e) and (f), the magnitude and

distribution of the vorticity near the trailing edge of the blades at different moments are almost the same. Besides, the maximum of the vorticity is located in the range from 1/3 to 1/2 of the span on the suction side of the blades and exceeds 2.4×10^4 s^{-1}. The minimum of the vorticity between the adjacent blades is closed to 2.0×10^3 s^{-1}. By comparing Fig. 20(a), (c), (e) and Fig. 20(b), (d), (f), it is found that the vorticity variations for the optimal unequally spaced fan and the prototype fan near the trailing edge of the blades are similar in their rotational process.

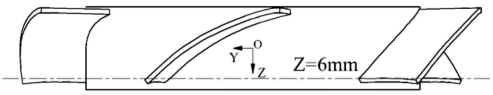

Fig. 19 Section Z = 6 mm (Near the trailing edge of blades).

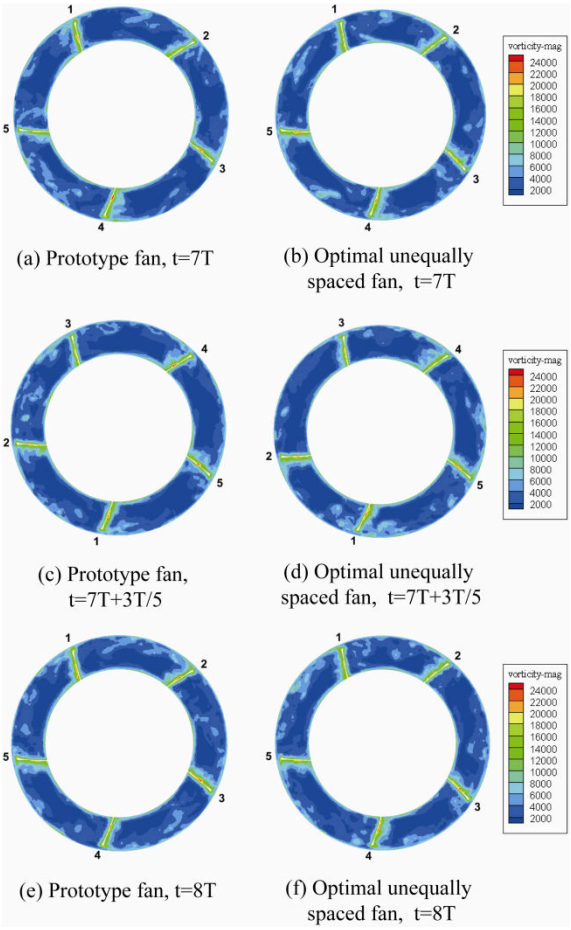

Fig. 20 Vorticity contours at the section Z = 6 mm at different moments.

In summary, the lower discrete noise of the optimal unequally spaced fan at the near field monitoring can be explained by the more regular fluctuation of total pressure. While the differences of broadband noise between the optimal unequally spaced fan and the prototype fan at the far field monitoring point are very little mainly because the magnitude, the distribution and the variation of vorticity of both fans near the trailing edge of the blades are almost the same.

Noise experiment

In order to verify the reliability of the simulation results for aerodynamic noise, noise experiment of the optimal unequally spaced fan and the prototype fan was carried out in a semi-anechoic room whose structure size was 5 m × 4 m × 3.5 m. The background noise is 21.5dB. The experimental device for noise measurement is shown in Fig. 21.

Fig. 22 shows the measured SPL along the axial direction in the downstream of fans. It can be seen that the largest difference of SPL between the optimal unequally spaced fan and the prototype fan is located at the near field measuring point that is 1mm away from the impeller hub in the axial direction. The value of largest difference exceeds 3dB. With the increase of the axial distance between the measuring point and the fan, SPL of both

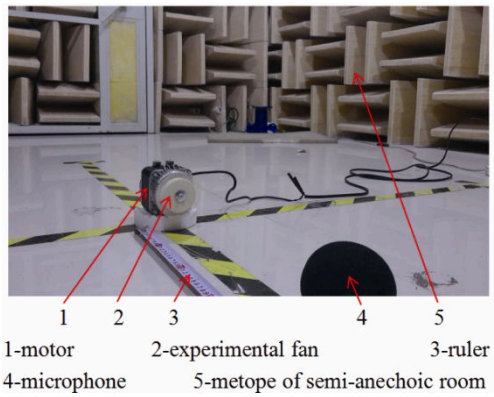

Fig. 21 Experimental device for noise measurement.

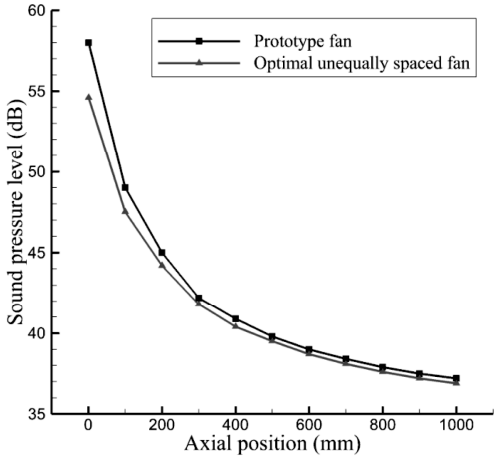

Fig. 22 Measured SPL along the axial direction in the downstream of fans.

fans decreases quickly at first, then the variation tends to be stable. The values of SPL of both fans are almost the same at the far field measuring point where is 1m away from the impeller hub in the axial direction.

The difference between experimental data and simulation results exists, mainly because the experimental fans don't have the casing. However, the experimental data of the optimal unequally spaced fan and the prototype fan have comparability. Through the noise experiment, it is further proved that the uneven circumferential blade space can reduce discrete noise of small axial flow fan obviously, but the effect on broadband noise is very little.

Conclusions

In this paper, the effects of the uneven circumferential blade space on the performance of a small axial flow fan are studied from two aspects including static characteristics and aerodynamic noise. Based on the prototype fan, blade angle modulation is adopted to design a series of unequally spaced fans with different $\Delta\theta$. The conclusions are summarized as follows:

(1) The simulation results show that the static pressure of the fans first increases and then decreases in general with the increase of $\Delta\theta$, while the efficiency of the fans decreases in general with the increase of $\Delta\theta$. The unequally spaced fan with $\Delta\theta = 6°$ has the optimal noise performance under the condition that the static characteristics can meet the requirement.

(2) The simulation and experiment show that the discrete noise of the optimal unequally spaced fan is lower than that of the prototype fan at the near field monitoring point, while the broadband noise of both fans is the same at the far field monitoring point.

(3) For the near field monitoring point, the noise is dominated by discrete noise. The total pressure fluctuation of the optimal unequally spaced fan is much more regular than that of the prototype fan. However, the magnitude and distribution of vorticity near the trailing edge of blades at different moments are almost the same for the compared two fans. Therefore, the total pressure fluctuation can be used to explain the reason why the discrete noise of the optimal unequally spaced fan is lower than that of the prototype fan.

(4) For the far field monitoring point, the noise is dominated by broadband noise and the noise caused by the variation of vorticity is much larger than that of the total pressure fluctuation. Due to the vorticity variations of both fans near the trailing edge of blades are similar in their rotational process, thus the broadband noise of both fans is close to each other.

Acknowledgement

This work was supported by National Natural Science Foundation of China (No. 51276172), Public Welfare Technology Application Projects of Zhejiang Province (No. 2015C31002), Open Foundation of Zhejiang Provincial Top Key Academic Discipline of Mechanical Engineering and Zhejiang Sci-Tech University Key Laboratory (ZSTUME 01A04), and Zhejiang Province Science and Technology Innovation Team Project (2013TD18).

References

[1] Cattanei, A., Ghio, R., Bongiovì, A.: Reduction of the Tonal Noise Annoyance of Axial Flow Fans by Means of Optimal Blade Spacing, Applied Acoustics, vol.68, pp.1323−1345, (2007).

[2] Mellin, R. C., Sovran, G.: Controlling the Tonal Characteristics of the Aerodynamic Noise Generated by Fan Rotors, Journal of Fluids Engineering, vol.92, pp.143−154, (1970).

[3] Wright, S. E.: Sound Radiation from a Lifting Rotor Generated by Asymmetric Disc Loading, Journal of Sound and Vibration, vol.9, pp.223−240, (1969).

[4] Sun, X.: The Aeroacoustic Nature of Unequally Spaced Fan, Journal of Beijing Institute of Aeronautics and Astronautics, vol.4, pp.137−145, (1986).

[5] Cui, C.: Analysis of Revolving Noise of Mine Fans with Uneven Blade Spacing, Mining & Processing Equipment, vol.38, pp.25−28, (2010).

[6] Xu, J.: Discussion on Fan Motor with Unequal Spaced Blades, Motor technology, vol.1, pp.7−10, (1987).

[7] Lévy, S.: Theoretical Study of the Acoustic Benefits of an Open Rotor with Uneven Blade Spacings, Journal of the Acoustical Society of America, vol.92, pp.2181−2185, (1992).

[8] Dobrzynski, W.: Propeller noise reduction by means of unsymmetrical blade-spacing, Journal of Sound and Vibration, vol.163, pp.123−136, (1993).

[9] Ewald, D., Pavlovic, A., Bollinger, J. G.: Noise reduction by applying modulation principle, Journal of the Acoustical Society of America, vol.49, pp.1381−1385, (1971).

[10] Duncan, P. E., Dawson, B.: Reduction of Interaction Tones from Axial Flow Fans by Suitable Design of Rotor Configuration, Journal of Sound and Vibration, vol.33, pp.143−154, (1974).

[11] Fiagbedzi, Y. A.: Reduction of Blade Passage Tone by Angle Modulation, Journal of Sound and Vibration, vol.82, pp.119−129, (1982).

[12] Roger, M.: Contrôle du Bruit Aérodynamique des Machines Tournantes Axiales par Modulation de Pales, Acoustica, vol.80, pp.247−259, (1994)